15. BAM-PTB Kolloquium vom 21.-22. Mai 2019 in Braunschweig
DOI: 10.7795/210.20190521P

Simulation of Explosion Hazards in Powder Flows

Holger Grosshans

Physikalisch-Technische Bundesanstalt, Fachbereich 3.5, Analyse & Simulation im Explosionsschutz, Braunschweig

Abstract

Conveying of powders gives rise to hazards to the operational safety of industrial facilities which caused numerous dust explosions in the past. The underlying physical mechanisms are often complex, inter-disciplinary, challenging to observe experimentally, and, thus, not well understood. To facilitate thorough theoretical analysis we have developed a computational tool which focuses specifically on the modeling of processes which may lead to ignition sources. This involves in particular the triboelectric charging of particles and piping components and the formation of deposits on surfaces. The first version of the resulting tool, called pafiX, was recently released for free download on the PTB website.

Keywords: *particle-laden flows, explosion protection, pafiX*

1 Introduction

Experience has shown that ignition and explosion can occur wherever powders are handled or permitted to accumulate which caused, despite precautions, numerous accidents in the past. As regards the pneumatic conveying of powders in the chemical and process industry, Eckhoff [1] has given in his standard textbook an overview over the associated safety risks. One of these risks arises from the occurrence of dust deposits on flown-through components, e.g. pipe and duct walls. These deposits can under certain conditions develop high temperatures and even internal smoldering fires, thereby serving as an ignition source for dust explosions. This is promoted by the porous structure of the deposits, which allows atmospheric oxygen to access the particle surfaces within the entire formation. At the same time the porosity reduces the thermal conductivity of the deposit, which prevents the dissipation of heat and leads to an increase in temperature in the event of an internal chemical reaction. This reaction may for example be caused by hot particles or heating of the transport component by an external source such as sunlight or welding. As long as sufficient oxygen is available, the reaction is further fanned and an ignition source is created. Another danger arises from the triboelectric charge exchange between particles and component surfaces during their contact. Excessive charging of the complete powder can lead to spark discharges, which have caused many explosions in the past [2].

Experimental tests in explosion protection are usually time-consuming, costly and always carry a certain risk potential. On the other hand, computing capacities are steadily becoming cheaper and constantly being expanded, also in the High Performance Computing (HPC) Section (Q.45) in PTB. Therefore, numerical simulations today offer a promising alternative to traditional research methods. Simulation is also characterized by the almost unlimited availability of spatially and temporally highly-resolved data. This is a particular advantage in the analysis of high temperature and pressure processes, which are often difficult to measure experimentally. The challenge in numerical simulation lies in the mathematical description of these processes and in the development of suitable numerical methods to accurately and effectively solve the resulting systems of equations.

The particular complexity of the numerical description of these processes arises from the interplay of different scientific disciplines, fluid mechanics (turbulent flow of the conveying air),

DOI: 10.7795/210.20190521P

surface science (triboelectric charge exchange, adhesion), electromagnetism (electrostatic attraction of charged particles) and chemistry (ignition and combustion). Because of this complex interaction, the fundamental mechanisms of this kind of flow are still not understood. Moreover, the coupling of the underlying field equations, which is a system of partial linear and non-linear differential equations, is extremely challenging.

Today, a wide range of simulation tools is on the market through which the dynamics of particle-laden flows can be computed. These include commercial tools such as ANSYS Fluent [3] or COMSOL Multiphysics [4], open source codes such as OpenFOAM [5] or Gerris [6] and a large number of academic in-house codes established at various research institutions. Despite their doubtless excellent capabilities to predict a wide range of different flows, none of these tools focuses on issues with specific importance for explosion protection. Moreover, most of their exhaustive features are not of relevance for the field of explosion protection which results in a steep learning curve for the end user.

Therefore, we currently establish a new computational tool called pafiX which abbreviates *particle flow simulation in explosion protection*. The aim of this tool is to provide a complete integral mathematical framework which facilitates the evaluation of risks associated with powder handling. Further, pafiX aims to be be fast to learn compared to other codes. It intends to be both a learning tool for basic research and enable the introduction of reasonable assumptions which will allow the establishment of a productive tool to provide fast results.

The following sections gives an overview over the mathematical model and numerical strategy of pafiX. Section 3 exemplifies some results to demonstrate the capabilities of the software and section 4 discusses the perspectives for future developments.

2 pafiX – particle flow simulation in explosion protection

In order to answer the demand for theoretical analyses of processes relevant for explosion protection during the industrial handling of powders, we have developed in collaboration with UC Louvain the tool pafiX (logo see figure 1). This tool is based on our experience and advancement of the numerical modeling of dispersed flows during the last decade. However, pafiX is a completely rewritten and restructured code, aiming to be efficient and at the same time as simple and understandable as possible. To give a rough idea, the simplification and removal of redundant features of our academic code as used e.g. for the studies documented in references [7, 8] led to the reduction of approximately 90% of lines of code. The compiled executables of pafiX are distributed through our group's website (`http://www.ptb.de/cms/asep`, follow the link to *software*). The first official release was in March 2019 and regular updates respectively addition of models and features are foreseen. This section outlines the mathematical model and numerical methods of the electrohydrodynamic (EHD) solver followed by an overview over the currently available models with specific relevance for explosion protection. It is noted that not all of these models may be available in the released version yet.

Figure 1: pafiX logo.

2.1 Mathematical model and numerical methods of the EHD solver

The equation system of the EHD solver consists of three strongly coupled parts, namely (i) the Navier-Stokes equations describing the evolution of the carrier gas, (ii) the electrostatic approximation of Maxwell's equations which characterize the electric field and (iii) Newton's laws of motion governing the dynamics of the particles.

DOI: 10.7795/210.20190521P

The Navier-Stokes equations, i.e. the continuity and momentum conservation equations for incompressible fluids, read

$$\nabla \cdot \boldsymbol{u} = 0 \tag{1a}$$

$$\frac{\partial \boldsymbol{u}}{\partial t} + (\boldsymbol{u} \cdot \nabla)\boldsymbol{u} = -\frac{1}{\rho}\nabla p + \nu \nabla^2 \boldsymbol{u} + \boldsymbol{F}_\mathrm{s}\,. \tag{1b}$$

Herein denotes $\boldsymbol{u}$ the velocity, ρ the density, p the pressure and ν the kinematic viscosity of the fluid. $\boldsymbol{F}_\mathrm{s}$ is a source term accounting for the momentum transfer from the particles to the fluid.

Furthermore, the electric field, $\boldsymbol{E}$, is solved by Gauss's law, which results from the electrostatic approximation of the Maxwell equations, given by

$$\nabla \cdot \boldsymbol{E} = \frac{\rho_\mathrm{el}}{\varepsilon}\,. \tag{2}$$

In this equation ρ_el is the electric charge density and ε the electrical permittivity of free space. If no external electric field is present, the electric charge density results directly from the positions of the individual particles and their individual charge.

The position of the particles is calculated in the Lagrangian frame of reference, i.e. for every particle the second Newtonian law is solved,

$$\frac{\mathrm{d}\boldsymbol{u}_\mathrm{p}}{\mathrm{d}t} = \boldsymbol{f}_\mathrm{ad} + \boldsymbol{f}_\mathrm{coll} + \boldsymbol{f}_\mathrm{g} + \boldsymbol{f}_\mathrm{el}\,. \tag{3}$$

Here, $\boldsymbol{f}_\mathrm{ad}$ is the acceleration of the particle by the attacking aerodynamic force, $\boldsymbol{f}_\mathrm{coll}$ by collisions, $\boldsymbol{f}_\mathrm{g}$ by gravitation and $\boldsymbol{f}_\mathrm{el}$ by electric field forces. The last term is calculated as

$$\boldsymbol{f}_\mathrm{el} = \frac{Q\boldsymbol{E}}{m_\mathrm{p}} \tag{4}$$

where Q is the charge and m_p is the mass of the particle.

A well-known problem in the solution of the Navier-Stokes equations is the lack of an independent equation for the pressure. Moreover, for incompressible flows mass conservation is more a kinematic constraint than a dynamic equation. This complication is overcome by coupling the continuity and momentum equations through the distributed Gauss-Seidel scheme proposed by Brandt and Dinar [9], which is herein extended to three-dimensional domains and non-uniform grids. The idea of this scheme is to diminish the error in the continuity equation by adjusting the velocity field. Afterward, the pressure field is adapted accordingly so that the residuals of the momentum equation at all points remain unchanged. Distributive relaxation represents an efficient and intuitive alternative to more widespread schemes such as SIMPLE or PISO.

The numerical solution of those of the above equations which are formulated in an Eulerian framework (equations (1a-2) requires the discretization of the derivatives on a numerical grid. In detail, the convective term is approximated by up to fifth-order accurate Weighted Essentially Non Oscillatory (WENO) schemes [10], the diffusive terms, the pressure terms and the mass conservation equation by fourth-order central differences, the divergence of the electric field by second order central differences, and the time derivatives by an implicit second-order backward scheme. Further, to reduce the required memory and computing costs the deferred-correction method is applied. In this method, the numerical approximation of a term ϕ is expressed by

$$\phi = \phi^\mathrm{l} + \left(\phi^\mathrm{h} - \phi^\mathrm{l}\right)^\mathrm{old} \tag{5}$$

where the superscript l denotes an approximation by a low-order scheme and h by a high-order scheme. The terms indicated by 'old' are computed explicitly using values from the previous time-step.

DOI: 10.7795/210.20190521P

To avoid odd-even decoupling between the pressure and velocity, which leads to the checkerboard problem, a staggered grid is used. More specifically, the variables p, $\boldsymbol{E}$ and ρ_{el} are computed at the cell center whereas the velocity components and the source term are calculated at the center of the cell faces. The resulting linear system of equations is solved using the Jacobi method which facilitates straight-forward parallelization of the code. As regards the direction of the sweep over the domain, symmetric relaxation is chosen [9]. This means that in the first pass the sweep is taken in increasing order of the cell indices, and in the second pass the order is reversed.

2.2 Modeling relevant for explosion protection

2.2.1 The condenser model for particle charging

To predict the charging of individual particles a wide-spread model, the so-called *condenser model*, is implemented in pafiX. Its name refers to the analogy of the process to the temporal response of a capacitor (also known as condenser) in a resistor-capacitor (R-C) circuit. In general, the model is restricted to conductive particles, i.e. a uniformly distributed charge distribution on the surface of the particles is assumed. Thus, this approach is referred to as *uniform-charge model*. The original formulation of the condenser model by Soo [11] aimed at the computation of the charge exchange between two colliding solid spheres. According to this formulation, no charge exchange due to different contact potential takes place during collisions if both particles are of the same material. This situation is expected for particles being part of the same homogeneous powder batch. Nevertheless, charge exchange may take place if at least one of the involved particles carries charge prior to the contact. Then, the charge transfer between two particles, $\Delta Q_n = -\Delta Q_m$, during the collision contact time, Δt_{p}, is given by, [11],

$$\Delta Q_n = \frac{C_n C_m}{C_n + C_m} \left(\frac{Q_m}{C_m} - \frac{Q_n}{C_n} \right) \left(1 - \mathrm{e}^{-\Delta t_{\mathrm{p}}/\tau_{\mathrm{p}}} \right) = -\Delta Q_m \,. \tag{6}$$

In the above equation, C_n and C_m denote the capacity of both particles and τ_{p} their charge relaxation time.

This model was expanded by John et al. [12] to compute the impact of a spherical particle with a plane surface such as a wall or a plate. In opposite to particle-particle collisions, in this situation the two objects in contact are usually of a dissimilar material. Thus, the total impact charge from the target to the particle, ΔQ, is given by the sum of the dynamic charge transfer to the particle caused by the contact potential, ΔQ_{c}, and the transferred pre-charge, ΔQ_{t}, i.e.,

$$\Delta Q = \Delta Q_{\mathrm{c}} + \Delta Q_{\mathrm{t}} \,. \tag{7}$$

The dynamic charge transfer during the wall-particle contact time Δt_{pw} is (as for a parallel plate condenser) given by

$$\Delta Q_{\mathrm{c}} = -C V_{\mathrm{c}} \left(1 - \mathrm{e}^{-\Delta t_{\mathrm{pw}}/\tau_{\mathrm{pw}}} \right) \tag{8}$$

where C is the electrical capacity, V_{c} is the contact potential between the particle and the target and τ_{pw} the charge relaxation time.

As mentioned above, it is commonly assumed [12, 13] that the pre-charge is distributed uniformly on the particles surface. Further, if the charge within the particle-target contact area, A_{pw}, is completely transferred, ΔQ_{t} equals for a particle of the radius r

$$\Delta Q_{\mathrm{t}} = -\frac{A_{\mathrm{pw}}}{4\pi r Q_n} \,. \tag{9}$$

DOI: 10.7795/210.20190521P

2.2.2 Model of non-uniform particle charging

The above discussed condenser model is only valid for particles of conductive surfaces. To account for the charge distribution on the surface of non-conductive particles, we extended this model to the *non-uniform charge model* [14] and implemented it in pafiX.

In the new formulation, instead of integral quantities, the local charge transfer, dq, per infinitely small surface element, s, of the particle is resolved. More precisely, during the collision of two particles (n and m) the local charge exchanges $dq_n(s_n)$ and $dq_m(s_m)$ on the surface elements s_n and s_m, respectively, during the particle-particle contact time Δt_p are given by

$$dq_n(s_n) = \frac{C_n C_m}{C_n + C_m} \left(\frac{dq_m(s_m)}{C_m} - \frac{dq_n(s_n)}{C_n} \right) \left(1 - \mathrm{e}^{-\Delta t_\mathrm{p}/\tau_\mathrm{p}} \right) = -dq_m(s_m)\,. \tag{10}$$

As regards the contact between a particle and a target (e.g. a plate or a wall), the non-uniform charge model also resolves the local charge transfer, dq, at an infinite small surface element, s, of the particle as

$$dq(s) = dq_\mathrm{c}(s) + dq_\mathrm{t}(s)\,. \tag{11}$$

Analogous to the uniform model, in this equation dq_c and dq_t denote the dynamic charge transfer at the surface spot s and the transfer of local pre-charge, respectively. It is assumed that only the pre-charge which is located at s is transferred, i.e.,

$$dq_\mathrm{t}(s) = -q_n(s)\,. \tag{12}$$

Moreover, the total dynamic charge exchange is defined as the integral of its density over the particle/wall contact area, A_pw, namely

$$\int\limits_{A_{pw}} dq_\mathrm{c}(s) = \Delta Q_\mathrm{c}\,. \tag{13}$$

As regards the numerical solution of the above equations, the surface is discretized into a finite number of surface spots, n_sides, which each can carry charge. In other words, the surface element s in equations (10)-(13) becomes a discrete quantity. Simplifying assumptions include that the location of the contact surface on the particles' surface is randomly determined. Moreover, the contact area is assumed to be symmetric around its center.

The precise derivation of the variable properties in the above equations and their detailed the numerical solution procedure are given in reference [14].

2.2.3 Formation of particle deposits and agglomerations

The modeling of the adhesion process and the formation of deposit layers on surfaces is part of our current research. Corresponding numerical methods are developed within a project funded by the Max Buchner Research Foundation of DECHEMA. The model presented in reference [15] is outlined in the following. The sticking of particles to surfaces or to each other poses constraints to the future particle dynamics. Numerically, a number is assigned to each particle cluster whereas "free" particles are assigned to a pseudo cluster 0, see figure 2.

Particles belonging to the same cluster impose contact forces on each other. Since the number of possible contact points within one cluster scales with $(N^2+N)/2$ (where N is the number of contained particles) the problem of solving the particle trajectories becomes fast numerically impossible when the cluster grows. To overcome this problem, we extended the approach of

DOI: 10.7795/210.20190521P

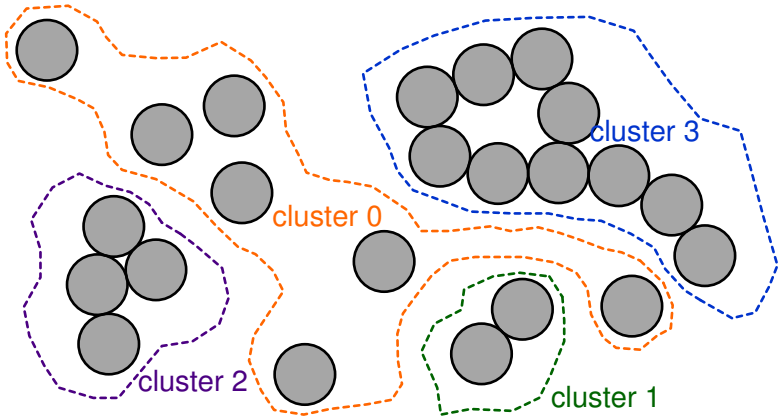

Figure 2: Some particles agglomerate (cluster 1-3) which severely constraints their dynamics whereas "free" particles are assigned to a pseudo cluster 0 [15].

Erleben [16] where the momentum equation for each particle belonging to a cluster, discretized using an explicit Euler scheme, becomes

$$\vec{u}^{t+1} = \vec{u}^{t} + \boldsymbol{M}^{-1}\boldsymbol{J}^{T}\Delta t\vec{\lambda} + \Delta t\boldsymbol{M}^{-1}\,\vec{f}_{\text{ext}}^{\,t}\ . \tag{14}$$

In this equation, the second term on the right hand side represents the kinematic constraints posed by the particles belonging to the same cluster. The last term sums up all external forces, which are the ones given in equation 3 and, additionally, attractive van der Waals forces.

Van der Walls forces between two spherical particles in close proximity are computed adopting the model of Hamaker [17],

$$F_{\text{vdW,pp}} = -A_{\text{H}}\frac{32}{3}\frac{r_n^3 r_m^3 (r_n + r_m + a)}{(2r_n + a)^2(2r_m + a)^2(2r_n + 2r_m + a)^2 a^2} \tag{15}$$

where a the distance between the surfaces of the particles and A_{H} is the Hamaker-Constant. The equivalent expression for the forces between a spherical particle and a plane surface was derived by Hartmueller and Ripperger [18], by letting r_m go to infinity which yields

$$F_{\text{vdW,ps}} = \lim_{r_m \to \infty} F_{\text{vdW,ps}} = -\frac{2}{3}\frac{A_{\text{H}}}{(2 + a/r_m)^2\, a/r_m}\,. \tag{16}$$

In both equations the minimal distance is limited by $a \geq 1\,\text{Å} = 10^{-10}\,\text{m}$.

3 Exemplary results

The developed tool has been used in the past years to perform manifold studies regarding a wide range of issues related to particle-laden flows. For example, in reference [8] the influence of electrostatic charges on the emerging flow pattern was elucidated. These investigations were performed in a generic geometry relevant to real-world applications in process engineering, a square-section tube. The resulting time-averaged particle distributions are illustrated for the case of an uncharged powder in figure 3(a). It is evident that the particles reside preferably close to the wall and especially in the corners of the pipes, while the particle density in the middle of the pipe is rather low. This phenomenon is known as *turbophoresis*, the migration of particles into flow regions with less turbulence. Surprisingly, the particle concentration in the

DOI: 10.7795/210.20190521P

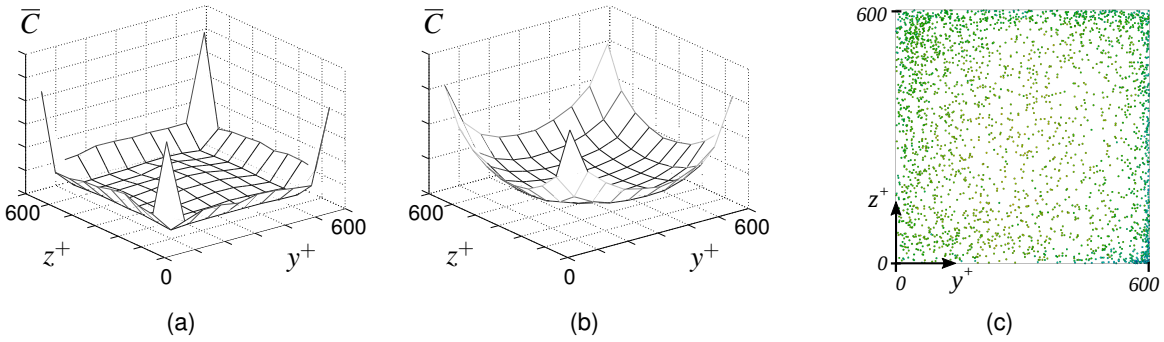

Figure 3: (a,b) Momentary and (c) time-averaged ($\overline{C}$) particle distribution in a square duct. The particles in (a) are uncharged whereas in (b) and (c) each particles carries 1 pC (reprinted from Ref. [19]

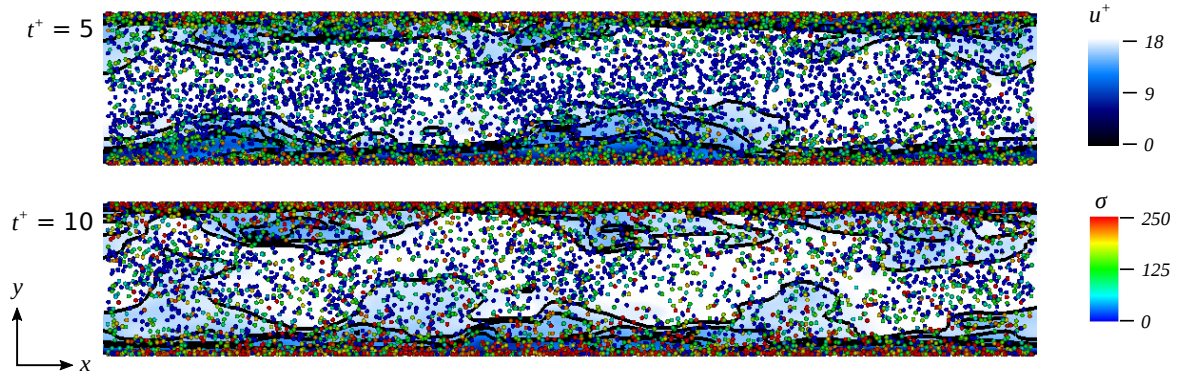

Figure 4: Instantaneous visualizations of the flow patterns of the case of $Ri = 0$, $U = 1$, $St = 20$ and $\omega = 0.23 \cdot 10^{-6}$. The black contours represent the isolines of the magnitude of the fluid velocity. For visualization purposes, the particles are enlarged and only every other particle is shown. The x-axis points to the streamwise direction and the y-axis to the wall-normal direction (reprinted from Ref. [7]).

near-wall regions is reduced when a charge of 1 pC is applied to the particles, see figure 3(b). This can be explained by the fact that charge of the same polarity was applied to all particles which leads to repulsive inter-particle forces. These forces are particularly strong in the areas where the mean distances between the particles are low, i.e. those with the highest particle density. The particles are pushed out of the high density areas and migrate towards the center of the duct. In this study also induced mirror charges on the tube surface were considered, which contribute to the attraction of the particles to the surface. However, these were found to be negligible compared to the repulsive forces between particles. Although the assumption of a powder of homogeneous polarity represents a special case, it is nonetheless of practical relevance since charge transfer in the same direction during wall contact is to be expected according to the triboelectric voltage series for particles of the same material. It is also interesting that the particle distribution in the time average is symmetrical to the planes of symmetry of the pipe cross-section, but the particle positions at a certain time can be quite strongly asymmetric. This is shown in snapshot 3(c), where the particles accumulate, especially in the lower right corner. As the particles progress, they continue to fill in the other corners.

In the simulations described above, the charge of the particles was assumed to be constant over time. In contrast, the computation of the particle charging process, which was documented

DOI: 10.7795/210.20190521P

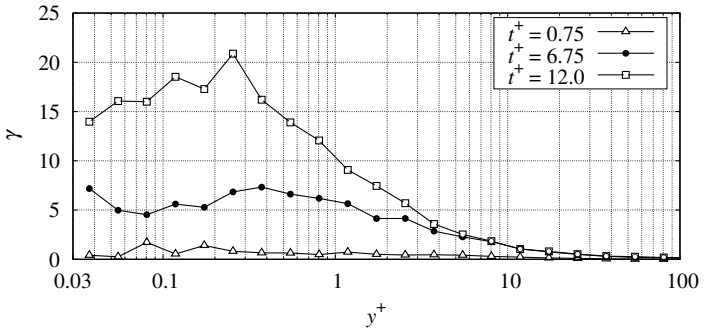

Figure 5: Evolution of the profiles of the linear charge density γ for the case of $Ri = 0$, $U = 1$, $St = 20$ and $\omega = 0.23 \cdot 10^{-6}$. At high Stokes numbers, a significant amount of electric charge migrates towards the centerplane of the channel via particle-bound charge transport (reprinted from Ref. [7]).

in publication [7] for a turbulent channel flow, is undoubtedly more difficult. Two exemplary instantaneous flow-fields for the conditions $Ri = 0$, $St = 20$, $\omega = 0.23 \cdot 10^{-6}$, and $U = 1$ are depicted in figure 4. Herein, t^+ is the physical time non-dimensionalized with the friction velocity and the half-width of the channel. A Richardson number, Ri, of zero means that gravity is neglected. The Stokes number, St is the ratio of the particle response time scale to a characteristic flow time scale. Further, ω denotes the volume fraction of the particulate phase. Finally, U is the contact potential non-dimensionalized by a reference potential U_0 that is set equal to 1 V.

In figure 4 the particle charge is expressed in terms of the absolute non-dimensional specific charge σ. Figure 4 indicates that the particles in the vicinity of the walls carry, on average, the highest charge whereas the number of charged particles in the bulk of the flow increases with time. This implies that the particles accumulate charge during wall collisions and subsequently migrate towards the center of the channel which is referred to as *particle-bound charge transport*. Thus, particle-bound charge transport and turbophoresis are counter-acting mechanisms, as regards the charging patterns and distribution of electric charge across the channel.

In contrast, for the conditions presented in figure 4 but a low Stokes number, $St = 0.2$, the particles follow closely the flow streamlines and the amount of electric charge accumulated by the particles is negligible. When the Stokes number was increased to 2 while keeping the other parameters constant the location of the peak value of the particles' number density is significantly shifted towards the wall. This results in a sufficiently high particle-wall collisions frequency to cause significant particle electrification. The particles get charged at the wall but, due to low particle dynamics, the electric charge remains confined within a thin layer close to the wall. More specifically, throughout the duration of the simulation, most of the electric charge is still located in the viscous sublayer.

In the case of a high Stokes number, $St = 20$, the charging rate of particles is significant increased. Here, the momentum of these particles in the wall-normal direction is sufficient to cross the viscous sublayer without getting trapped by the near-wall structures of the flow. This causes a different charge distribution and at $t^+ = 12$ the peak of γ is detached from the wall, see in figure 5. Moreover, a significant amount of charge is transported due to their inertia towards the bulk of the channel via particle-bound transport.

Finally, first results regarding particle agglomeration are presented in figure 6. Two scenarios of the time evolution of colliding particles are depicted. Both scenarios are computed for identical conditions, with the exception that the two particles in the bottom are subjected to van der Waals forces. Initially, the red particles propagates with a velocity of 0.1 m/s in x-direction towards the blue particles which are still. All particles are of a diameter of 2 mm and a restitution ratio of 0.6. The blue particles are shifted by -1 mm in y-direction compared to the red particles, so a

DOI: 10.7795/210.20190521P

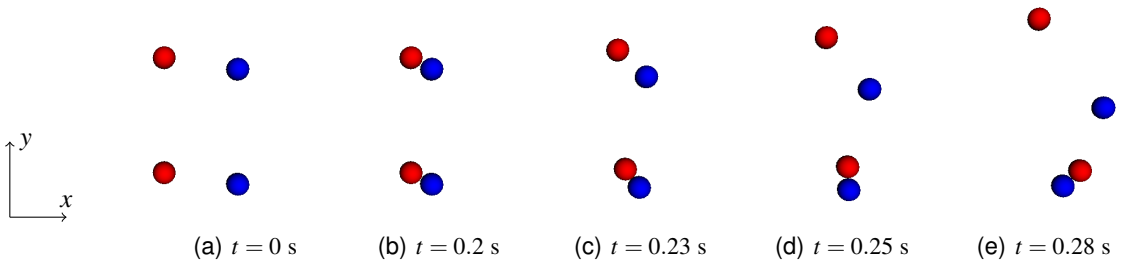

Figure 6: Snapshots of the time evolution of two colliding particles. In the bottom scenario the particles stick to each other due to van der Waals forces [15].

two-dimensional collision is expected. In the top scenario the particles collide and reflect each other at $t = 0.02$ s. The red particle evolves upwards and the blue particle downwards. In the bottom scenario, sufficient kinetic energy is dissipated that the van der Waals forces keep both particles attached to each other. In the further evolution it can be observed how both particles stick to each other and rotate around a common center. This represents the first step of the formation of a particle agglomeration.

4 Perspectives

In summary, we have made significant progress in the modeling of particle-laden flows in recent years. However, this research is still in its beginning, especially the computation of the processes of deposition formation and particle charging are major challenges. The solution of these problems through new, interdisciplinary approaches will in the future contribute to the safe handling of powders and operation of industrial plants. The first version of pafiX was recently released but will require constant updates and future improvements. The intended improvements aim to reduce the computational time through the establishment of a Reynolds-Averaged Navier-Stokes (RANS) approach for the gaseous phase and an Eulerian description of the particulate phase. Moreover, the distribution of the code as open source, the possibility to model more complex geometries and other features are an option.

Acknowledgements

The author gratefully acknowledges the financial support from the Max Buchner Research Foundation and G. Lindner (PTB, Berlin) for the support during the usage of the compute cluster.

References

[1] Eckhoff, R. K. (2003). *Dust Explosions in the Process Industries*. Gulf Professional Publishing, 3rd edition.

[2] Egan, S. (2017). *Learning lessons from five electrostatic incidents*. J. Electrostatics, 88:183–189.

[3] ANSYS Fluent (2018). Release 18.1, Academic Research Mechanical.

[4] COMSOL Multiphysics (2018). `http://www.comsol.com`. COMSOL AB, Stockholm, Sweden.

DOI: 10.7795/210.20190521P

[5] Weller, H. G., Tabor, G., Jasak, H., and Fureby, C. (1998). *A tensorial approach to computational continuum mechanics using object-oriented techniques*. Comput. Phys., 12:620–631.

[6] Popinet, S. (2003). *Gerris: a tree-based adaptive solver for the incompressible Euler equations in complex geometries*. J. Comp. Phys., 190:572–600.

[7] Grosshans, H. and Papalexandris, M. V. (2017). *Direct numerical simulation of triboelectric charging in a particle-laden turbulent channel flow*. J. Fluid Mech., 818:465–491.

[8] Grosshans, H. (2018). *Modulation of particle dynamics in dilute duct flows by electrostatic charges*. Phys. Fluids, 30(8):083303.

[9] Brandt, A. and Dinar, N. (1978). *Multigrid solutions to elliptic flow problems*. In *Numerical Methods for Partial Diffential Equations*. The University of Wisconsin-Madison.

[10] Jang, G. S. and Shu, C. W. (1996). *Efficient implementation of weighted ENO schemes*. J. Comput. Phys., 126:202–228.

[11] Soo, S. L. (1971). *Dynamics of charged suspensions*. In *Topics in Current Aerosol Research*, pages 71–73. Pergamon Press.

[12] John, W., Reischl, G., and Devor, W. (1980). *Charge transfer to metal surfaces from bouncing aerosol particles*. J. Aerosol Sci., 11(2):115–138.

[13] Kolniak, P. Z. and Kuczynski, R. (1989). *Numerical modeling of powder electrification in pneumatic transport*. J. Electrostat., 23:421–430.

[14] Grosshans, H. and Papalexandris, M. V. (2016). *A model for the non-uniform contact charging of particles*. Powder Technol., 305:518–527.

[15] Klahn, E. and Grosshans, H. (2019). *Modeling the agglomeration of electrostatically charged particles*. In *Electrostatics 2019, submitted*. Manchester, UK.

[16] Erleben, K. (2007). *Velocity-based shock propagation for multibody dynamics animation*. ACM Trans, 26:1–5. doi:10.1145/1243980.1243986.

[17] Hamaker, H. C. (1937). *The London-van der Waals attraction between spherical particles*. Physica, 4:1058–1072.

[18] Hartmueller, J. and Ripperger, S. (2014). *Die Haftung von Partikeln an Bauteiloberflächen*. Filtrieren und Separieren, 28:274ff.

[19] Grosshans, H. (2018). *Modulation of particle-laden flows by electrostatic charges*. In *12th International Symposium on Hazards, Prevention and Mitigation of Industrial Explosions*. Kansas City, MO, USA.